Z_2 gauge theory description of the Mott transition in infinite dimensions

Rok Žitko[1,2] and Michele Fabrizio[3]

[1]*Jožef Stefan Institute, Jamova 39, SI-1000 Ljubljana, Slovenia*

[2]*Faculty of Mathematics and Physics, University of Ljubljana, Jadranska 19, SI-1000 Ljubljana, Slovenia*

[3]*International School for Advanced Studies (SISSA) and CNR-IOM Democritos, Via Bonomea 265, I-34136 Trieste, Italy*

(Received 7 April 2015; revised manuscript received 29 May 2015; published 15 June 2015)

The infinite-dimensional half-filled Hubbard model can be mapped exactly with no additional constraint onto a model of free fermions coupled in a Z_2 gauge-invariant manner to auxiliary Ising spins in a transverse field. In this slave-spin representation, the zero-temperature insulator-to-metal transition translates into spontaneous breaking of the local Z_2 gauge symmetry, which is not forbidden in infinite dimensions, thus endowing the Mott transition of an order parameter that is otherwise elusive in the original fermion representation. We demonstrate this interesting scenario by exactly solving the effective spin-fermion model by dynamical mean-field theory both at zero and at finite temperature.

DOI: 10.1103/PhysRevB.91.245130 PACS number(s): 71.10.Fd, 71.30.+h, 05.30.Rt

I. INTRODUCTION

Sixty years after Sir Nevill Mott first envisaged it [1], the interaction driven metal-to-insulator (Mott's) transition remains an object of considerable efforts aiming at its full comprehension. The main difficulty resides in the inability of approximate methods based on independent particles to properly capture a transition that involves only part of electrons' degrees of freedom: their charge. This is frustrating since the common attitude is tracing back complex many-body phenomena to independent particle models, an approach on which many successful techniques are based, e.g., the mean-field theory or the density functional theory within the local density approximation.

A tool that has often been employed to disentangle charge from other electron quantum numbers, thus making Mott's localization accessible already at the mean-field level, is to associate local charge configurations to novel fictitious degrees of freedom. This requires supplemental local constraints in order to project the enlarged Hilbert space onto the physical one.

A well-known implementation of this idea is the *slave boson* technique [2,3]. The slave-boson mean-field theory is indeed able to describe the metal-insulator transition [4]. In this language, however, the Mott transition is associated with a local $U(1)$ gauge symmetry that is maintained in the insulator but spontaneously broken in the metal, which is physically not possible. Restoring the symmetry to assess how robust are the mean-field results requires adding quantum fluctuations, which is not an easy task [5–7].

In a recently proposed alternative route the slave bosons are replaced by slave Ising variables [8–11]. The advantage is that the size of the enlarged local Hilbert space is only a few times bigger than the physical one, not infinitely as in the slave-boson approach. In addition, the continuous $U(1)$ local gauge symmetry is replaced by a discrete Z_2 one.

Let us consider the single-band model

$$\mathcal{H} = -\sum_{i,j}\sum_{\sigma} t_{ij} c^{\dagger}_{i\sigma} c_{j\sigma} + \sum_i \frac{U_i}{4}\,[2(\hat{n}_i - 1)^2 - 1], \qquad (1)$$

where $\hat{n}_i = \sum_\sigma c^{\dagger}_{i\sigma} c_{i\sigma}$, and for later convenience, we added a constant term. The Hamiltonian $\mathcal{H}$ corresponds to the conventional Hubbard model when $U_i = U$, $\forall i$, and to the Anderson (Wolff) impurity model when $U_i = U$ for $i = i_0$ while $U_i = 0$ for any $i \neq i_0$, with the impurity sitting at i_0. The partition function Z corresponding to the Hamiltonian in Eq. (1) can be shown [11] to be equivalent to

$$Z = \mathrm{Tr}(e^{-\beta\mathcal{H}}) \equiv Z_* = \mathrm{Tr}\left(e^{-\beta\mathcal{H}_*}\prod_i \mathbb{P}_i\right), \qquad (2)$$

where the slave-spin Hamiltonian $\mathcal{H}_*$ is

$$\mathcal{H}_* = -\sum_{i,j}\sum_{\sigma} t_{ij}\sigma^x_i\sigma^x_j c^{\dagger}_{i\sigma} c_{j\sigma} - \sum_i \frac{U_i}{4}\,\sigma^z_i, \qquad (3)$$

with the Pauli matrices σ^a_i, $a = x,y,z$, describing auxiliary Ising spins, and the projection operator

$$\mathbb{P}_i = \frac{1}{2} + \frac{\sigma^z_i\,\Omega_i}{2}, \qquad (4)$$

with Ω_i defined as [see Eq. (1)]

$$\Omega_i = 1 - 2(\hat{n}_i - 1)^2. \qquad (5)$$

We observe that Ω_i has eigenvalue $+1$ when $\hat{n}_i = 1$ and -1 when $\hat{n}_i = 0$ or 2; this operator thus corresponds to charge fluctuations away from single occupancy of site i. Therefore $\mathbb{P}_i$ is actually a projector onto the physical Hilbert space defined by $\sigma^z_i = \Omega_i$. As anticipated, the Hamiltonian $\mathcal{H}_*$ possesses a local Z_2 gauge symmetry

$$\sigma^x_i \to s_i\sigma^x_i, \quad c^{\dagger}_{i\sigma} \to s_i c^{\dagger}_{i\sigma}, \qquad (6)$$

where $s_i = \pm 1$.

The equivalence of partition functions in Eq. (2) was proved by equating the perturbative expansion in U_i of Z with that of Z_* [11]. It was observed that the two terms that define the projector $\mathbb{P}_i$ in Eq. (4) have a very distinct role in perturbation theory [11]. Specifically, the first term $1/2$ accounts for all diagrams in the perturbation series where U_i is applied an even number of times, while the second term $\sigma^z_i\,\Omega_i/2$ takes care of all diagrams where U_i is instead applied an odd number of times.

This simple observation has a remarkable outcome. If Z is known to be an even function of some U_i, then the term $\sigma^z_i\,\Omega_i/2$ in Eq. (4) plays no role and can be discarded. This result can be easily proven even without resorting to the perturbation

theory. If $Z(U_i) = Z(-U_i)$, also $Z_*(U_i) = Z_*(-U_i)$. Since $\sigma_i^x\, \mathcal{H}_*(U_i)\sigma_i^x = \mathcal{H}_*(-U_i)$ and $\sigma_i^x\, \mathbb{P}_i \sigma_i^x = 1 - \mathbb{P}_i$, because the partition function is invariant under a unitary transformation it follows that

$$Z_*(U_i,\mathbb{P}_i) = Z_*(-U_i,\mathbb{P}_i) = Z_*(U_i,1-\mathbb{P}_i) = Z_*\left(U_i,\frac{\mathbb{P}_i+(1-\mathbb{P}_i)}{2}\right) = Z_*\left(U_i,\frac{1}{2}\right). \quad (7)$$

The fortunate event $Z(U_i) = Z(-U_i)$ occurs, in particular, at particle-hole symmetry in the Anderson impurity model, where the positive-U model maps onto the negative-U model through the partial partial-hole transformation

$$c_{i\uparrow}^\dagger \to d_{i\uparrow}^\dagger, \quad c_{i\downarrow}^\dagger \to (-1)^i d_{i\downarrow}. \quad (8)$$

This model exchanges the spin and charge degrees of freedom and transforms the spin Kondo effect into the charge Kondo effect [12–16].

Moreover, through the well-known dynamical mean-field theory (DMFT) mapping between an Anderson impurity model and a Hubbard model on a lattice with infinite coordination number [17], it follows that also the latter possesses this property at particle-hole symmetry. In other words, the partition functions of both models at the particle-hole symmetric point can be calculated through the partition function of the corresponding spin-fermion Hamiltonian $\mathcal{H}_*$ without any constraint.

This mapping was exploited for the Anderson impurity model in Ref. [18], where the equivalent spin-fermion Hamiltonian was solved by the numerical renormalization group (NRG) [19,20], unveiling the remarkable fact that the mean-field breaking of the local Z_2 gauge symmetry is not spurious: it actually occurs in the exact solution. In the same work it was also argued that a similar phenomenon might occur even in the Hubbard model on infinite-coordination lattices, where Elitzur's theorem [21] does not apply, hence a local Z_2 gauge symmetry can be spontaneously broken [22].

Our aim here is just to verify this conjecture and examine all its consequences. As a by-product, the reliable numerical solution of the lattice model, Eq. (3), provides the chance to assay how reliable is the mean-field approximation when applied to slave-spin models, at least in the case of lattices with infinite coordination number.

II. THE MODEL AND ITS MEAN-FIELD SOLUTION

The model we shall consider is the simple half-filled Hubbard model

$$\mathcal{H}_{\rm Hub} = -\frac{t}{\sqrt{z}}\sum_{\langle i,j\rangle}\sum_\sigma (c_{i\sigma}^\dagger c_{j\sigma} + {\rm H.c.}) + \frac{U}{4}\sum_i [2(n_i-1)^2 - 1], \quad (9)$$

with nearest-neighbor hopping on a Bethe lattice in the limit of infinite coordination number, $z \to \infty$. We focus on the fully frustrated case where the antiferromagnetic order does not appear and there is a Mott transition from a paramagnetic metal to a paramagnetic insulator. The phase diagram of the model is sketched in Fig. 1 [23]. The transition line between the metal and the Mott insulator is first order for $T > 0$ with a critical endpoint at $T_c \simeq 0.026D$ [24], where $D = 2t$ is half the bandwidth.

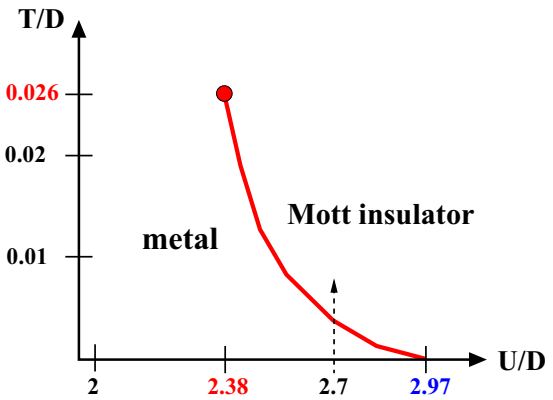

FIG. 1. (Color online) Sketch of the phase diagram of the paramagnetic half-filled Hubbard model on a Bethe lattice [23]. $D = 2t$ is half the bandwidth. At $U/D = 2.7$, the first-order metal-insulator transition occurs at the temperature $T \approx 0.0037D$.

As mentioned, the partition function of the Hubbard model $Z_{\rm Hub}$ can be also calculated through

$$Z_{\rm Hub} = \left(\tfrac{1}{2}\right)^N {\rm Tr}(e^{-\beta\mathcal{H}_{\text{s-f}}}), \quad (10)$$

where N is the number of sites and $\mathcal{H}_{\text{s-f}}$ is the spin-fermion Hamiltonian, Eq. (3), with $U_i = U, \forall i$, namely,

$$\mathcal{H}_{\text{s-f}} = -\frac{t}{\sqrt{z}}\sum_{\langle i,j\rangle}\sum_\sigma \sigma_i^x\sigma_j^x(c_{i\sigma}^\dagger c_{j\sigma} + {\rm H.c.}) - \frac{U}{4}\sum_i \sigma_i^z. \quad (11)$$

It follows that the spin-fermion model, Eq. (11), must also have the same phase diagram shown in Fig. 1.

The Hamiltonian $\mathcal{H}_{\text{s-f}}$ is invariant under the N mutually commuting unitary transformations $\sigma_i^z\,\Omega_i$, $\forall i$. Therefore we can divide the full Hilbert space into 2^N orthogonal subspaces identified by the sets of bits $\{n\} = (n_1,n_2,\ldots,n_i,\ldots,n_N)$, with $n_i = 0,1$, which contain states such that

$$\sigma_i^z\Omega_i|\psi_{\{n\}}\rangle = (-1)^{n_i}|\psi_{\{n\}}\rangle. \quad (12)$$

It follows that

$$Z_{\text{s-f}} = {\rm Tr}(e^{-\beta\mathcal{H}_{\text{s-f}}}) = \sum_{\{n\}} {\rm Tr}_{\{n\}}(e^{-\beta\mathcal{H}_{\text{s-f}}}) = \sum_{\{n\}} Z_{\text{s-f}\{n\}}, \quad (13)$$

where ${\rm Tr}_{\{n\}}$ stands for the trace within the invariant subspace $\{n\}$. All invariant subspaces are actually degenerate at particle-hole symmetry and in lattices with infinite coordination. Therefore $Z_{\text{s-f}\{n\}} = Z_*, \forall\{n\}$, so that $Z_{\text{s-f}} = 2^N Z_*$; a degeneracy that cancels out the prefactor in Eq. (10).

In view of the above result, it is worth briefly discussing the meaning of gauge symmetry breaking. We observe that, within each subspace, the matrix elements of any gauge-variant operator vanish. For instance,

$$\langle\psi'_{\{n\}}|\sigma_i^x|\psi_{\{n\}}\rangle = (-1)^{2n_i}\langle\psi'_{\{n\}}|\Omega_i\sigma_i^z\sigma_i^x\sigma_i^z\Omega_i|\psi_{\{n\}}\rangle = -\langle\psi'_{\{n\}}|\sigma_i^x|\psi_{\{n\}}\rangle,$$

hence $\langle\psi'_{\{n\}}|\sigma_i^x|\psi_{\{n\}}\rangle = 0$. Therefore, spontaneous gauge symmetry breaking can be revealed within each invariant subspace

only by the long-time behavior of gauge-invariant correlation functions, e.g., $\lim_{t\to\infty}\langle\sigma_i^x(t)\,\sigma_i^x(0)\rangle$. Alternatively, one can add to the Hamiltonian a test field that explicitly breaks the symmetry, and study the response in the limit of vanishing field.

A. Zero temperature

We shall start our analysis with a mean-field decomposition. At zero temperature, we assume a factorized variational state

$$|\Psi\rangle = |\text{Ising}\rangle \otimes |\text{fermions}\rangle. \tag{14}$$

The Ising wave function thus corresponds to the ground state of the Ising model in a transverse field

$$\mathcal{H}_{\text{Ising}} = -\frac{2}{z}\sum_{\langle i,j\rangle} J_{ij}\sigma_i^x\sigma_j^x - \frac{U}{4}\sum_i \sigma_i^z, \tag{15}$$

where, assuming translational symmetry,

$$\begin{aligned} J_{ij} &= \frac{t\sqrt{z}}{2}\sum_\sigma \langle\text{fermions}|c_{i\sigma}^\dagger c_{j\sigma} + \text{H.c.}|\text{fermions}\rangle \\ &= J, \quad \forall\langle i,j\rangle. \end{aligned} \tag{16}$$

In turn, $|\text{fermions}\rangle$ is the ground state of

$$\mathcal{H}_{\text{fermions}} = -\frac{t_*}{\sqrt{z}}\sum_{\langle i,j\rangle}\sum_\sigma (c_{i\sigma}^\dagger c_{j\sigma} + \text{H.c.}). \tag{17}$$

Here,

$$t_* = t\,\langle\text{Ising}|\sigma_i^x\sigma_j^x|\text{Ising}\rangle \tag{18}$$

does not depend on the specific nearest-neighbor bond as we have assumed translational symmetry.

It follows that $|\text{fermions}\rangle$ is just the Fermi sea of a tight-binding Hamiltonian with constant hopping. This implies that J in Eq. (16) has the value $J = 8t/3\pi$ independent of $|\text{Ising}\rangle$.

The Ising model in Eq. (15) with constant J can be readily solved on the Bethe lattice, where the mean-field results becomes exact for $z\to\infty$. In particular, one finds that, for any site i,

$$\left|\langle\text{Ising}|\sigma_i^x|\text{Ising}\rangle\right| = \theta(U_c - U)\sqrt{1-\frac{U^2}{U_c^2}}\,, \tag{19}$$

where $U_c = 8J$. Therefore, for $U < U_c$, the mean-field state has a finite order parameter that vanishes at U_c and above it. In the original model, Eq. (11), the finite value of $\langle\sigma_i^x\rangle$ actually implies that the local Z_2 gauge symmetry, Eq. (6), is broken. In fact, we observe that, given the variational wave function $|\Psi\rangle$ in Eq. (14), the state

$$|\Psi'\rangle = \prod_i \left(\sigma_i^z\Omega_i\right)^{m_i}|\Psi\rangle, \tag{20}$$

with $m_i = 0,1$, is also a solution of the mean-field equations with the same energy and is orthogonal to $|\Psi\rangle$. In fact, for $i\neq j$ the average value

$$\begin{aligned} \langle\Psi|\Omega_i\,\Omega_j|\Psi\rangle &= \langle\Psi|\Omega_i|\Psi\rangle\langle\Psi|\Omega_j|\Psi\rangle + O(z^{-2|i-j|}) \\ &\sim O(z^{-2|i-j|}), \end{aligned} \tag{21}$$

because the average of any Ω_i vanishes on the half-filled Fermi sea. Since for any given i there are z^r sites j at distance $|i-j| = r$, one readily concludes that $|\Psi\rangle$ and $|\Psi'\rangle$ are indeed orthogonal for $z\to\infty$. Therefore the mean-field lowest energy state is 2^N times degenerate, once more signaling the gauge symmetry breaking. Such degeneracy exactly compensates the entropic prefactor in Eq. (10), thus providing a physically meaningful variational estimate of the Hubbard model ground-state energy. We note that, on the insulating side where $t_* = 0$ [see Eq. (18)], the fermionic mean-field Hamiltonian in Eq. (17) vanishes, hence any wave function $|\text{fermions}\rangle$ solves the variational problem, leading to a degeneracy 4^N that is only partly compensated by the prefactor in Eq. (10). The net result is a residual entropy $S = N\,\ln 2$, which physically corresponds to the spin entropy of the hypothetical paramagnetic Mott insulator.

At first sight, the spontaneous symmetry breaking might look wrong by the Elitzur's theorem [21]. In reality, as we mentioned, this theorem does not apply in infinite-coordination lattices, where such a symmetry is not impeded from breaking spontaneously [22]. The phase with broken Z_2 gauge symmetry actually corresponds to a metal phase in the Hubbard model (9), while the phase at $U > U_c$ to the Mott insulator. Thence $U_c = 32/3\pi\,D \simeq 3.39D$ is the critical value of the Mott transition, which slightly overestimates the actual value $U_c \simeq 2.97D$ (see Fig. 1).

We mention that the zero-temperature mean-field solution is equivalent to the Gutzwiller approximation applied to the Hamiltonian, Eq. (9) [11,25], an approach that in fact provides exact results for the Gutzwiller wave function in infinite-coordination lattices [26,27]. The inclusion of quantum fluctuations on top of the mean-field solution is equivalent to the time-dependent Gutzwiller approximation [28]. Following Ref. [11], if we apply the spin-wave approximation to the Ising model by writing

$$\sigma_i^x \simeq \sin\theta\left(2 - x_i^2 - p_i^2\right) - \sqrt{2}\cos\theta\, x_i, \tag{22}$$

$$\sigma_i^z \simeq \cos\theta\left(2 - x_i^2 - p_i^2\right) + \sqrt{2}\sin\theta\, x_i, \tag{23}$$

$$\sigma_i^y \simeq \sqrt{2}\,p_i, \tag{24}$$

where x_i and p_i are conjugate variables and

$$\cos\theta = \begin{cases} U/U_c & \text{if} \quad U \leqslant U_c \\ 1 & \text{if} \quad U > U_c, \end{cases} \tag{25}$$

the Hamiltonian (15) becomes quadratic

$$\mathcal{H}_{\text{Ising}} \simeq E_0 + \frac{a}{2}\sum_i \left(x_i^2 + p_i^2\right) + \frac{b}{2}\frac{2}{z}\sum_{\langle i,j\rangle} x_i\,x_j, \tag{26}$$

where E_0 is the mean-field energy, $a = U_c/2$ and $b = U^2/2U_c$ for $U \leqslant U_c$, while $a = U/2$ and $b = U_c/2$ for $U > U_c$ [11]. The spin-wave spectrum is limited within the energy window $\omega_m \leqslant \omega \leqslant \omega_M$, where $\omega_M = \sqrt{a(a+b)}$ and

$$\omega_m = \sqrt{a(a-b)}. \tag{27}$$

In other words, the Ising excitations are gapped everywhere except at the Mott transition where $a = b$, close to which

$$\omega_m \simeq \frac{U_c}{2}\left|1-\frac{U}{U_c}\right|^{1/2}. \tag{28}$$

B. Finite temperature

The above mean-field approach can be extended to finite temperature without embarking into delicate issues related to gauge redundancy by simply exploiting the aforementioned equivalence with the Gutzwiller variational approach [25]. Within the latter scheme, one assumes for the original Hubbard model, Eq. (9), the density matrix

$$\rho_G = \mathcal{P}\rho_{\text{fermions}}\mathcal{P}^\dagger = \prod_i \mathcal{P}_i\,\rho_{\text{fermions}}\mathcal{P}_i^\dagger, \tag{29}$$

where ρ_{fermions} is the Boltzmann-Gibbs distribution of free fermions with nearest-neighbor hopping at half-filling, and the linear operator

$$\mathcal{P}_i = \frac{\Phi_\Uparrow}{\sqrt{2}}(1+\Omega_i) + \frac{\Phi_\Downarrow}{\sqrt{2}}(1-\Omega_i), \tag{30}$$

with $\Phi_\Uparrow$ and $\Phi_\Downarrow$ real variational parameters such that $\Phi_\Downarrow^2 + \Phi_\Uparrow^2 = 1$. We observe that $1+\Omega_i$ and $1-\Omega_i$ project onto states where site i is singly occupied and empty/doubly occupied, respectively. If we formally transform

$$\mathcal{P}_i \to \bar{\mathcal{P}}_i = \frac{\Phi_\Uparrow}{\sqrt{2}}[1+(-1)^{n_i}\Omega_i]|\Uparrow\rangle + \frac{\Phi_\Downarrow}{\sqrt{2}}[1-(-1)^{n_i}\Omega_i]|\Downarrow\rangle, \tag{31}$$

where $\sigma_i^z|\Uparrow(\Downarrow)\rangle = \pm|\Uparrow(\Downarrow)\rangle$, we realize that Eq. (31) applied on an electronic wave function generates a spin-fermion state belonging to the symmetry-invariant subspace with $\{n\} = (n_1, n_2, \ldots, n_i, \ldots, n_N)$ [see Eq. (12)]. Replacing $\mathcal{P}_i$ with $\bar{\mathcal{P}}_i$ in Eq. (29) yields a variational density matrix for the spin-fermion Hamiltonian, Eq. (11), restricted to the invariant subspace $\{n\}$:

$$\rho_G \to \rho_{\{n\}} = \prod_i \bar{\mathcal{P}}_i\,\rho_{\text{fermions}}\bar{\mathcal{P}}_i^\dagger. \tag{32}$$

Since at half-filling $\text{Tr}(\rho_{\text{fermions}}\Omega_i\sigma_i^z) = 0$, it follows that on the Bethe lattice with $z \to \infty$,

$$\text{Tr}\big(\rho_{\{n\}}\sigma_i^z\big) = \Phi_\Downarrow^2 - \Phi_\Uparrow^2 \equiv m$$

and

$$\text{Tr}\big(\rho_{\{n\}}\sigma_i^x c_{i\sigma}^\dagger \sigma_j^x c_{j\sigma}\big) = 4\Phi_\Uparrow^2\Phi_\Downarrow^2\,\text{Tr}(\rho_{\text{fermions}}c_{i\sigma}^\dagger c_{j\sigma}).$$

Both results are independent of $\{n\}$. This entails a renormalized hopping $t \to 4\Phi_\Uparrow^2\Phi_\Downarrow^2 t = (1-m^2)\,t$.

Following the finite-temperature calculations of Refs. [29] and [30] obtained within the Gutzwiller approximation, one ultimately has to minimize the free-energy density

$$\begin{aligned} F(m) = &-\frac{4T}{\pi D^2}\int_{-D}^{D} d\epsilon\sqrt{D^2-\epsilon^2}\,\ln(1+e^{-\beta(1-m^2)\epsilon}) \\ &-\frac{U}{4}(m-1) + T\,\ln 2 \\ &+T\left(\frac{1-m}{2}\ln\frac{1-m}{2} + \frac{1+m}{2}\ln\frac{1+m}{2}\right), \end{aligned} \tag{33}$$

where we recognize that the last term is just the entropy of a spin in a magnetic field $B = T\tanh^{-1}m$ directed along z. The phase diagram of Eq. (33) was calculated by the saddle-point method in Ref. [29] and agrees qualitatively with the exact one shown in Fig. 1.

Since the variational free-energy functional, Eq. (33), is the same for any of the 2^N subspaces $\{n\}$, such a degeneracy cancels the entropic prefactor in Eq. (10), bringing once again a free energy that is well defined in the thermodynamic limit. The above simple variational calculation is, however, unable to assess whether the symmetry is preserved or spontaneously broken. In Sec. III B we shall instead perform a numerically exact calculation at finite temperature to answer such question.

III. DMFT SOLUTION

In order to assess the validity of the mean-field approximation, we now move to the reliable numerical solution of the model, Eq. (11), by means of the DMFT using the NRG [19,20] to solve the impurity problem defined by

$$\mathcal{H}_{\text{imp}} = \sum_{\mathbf{k}\sigma}\epsilon_{\mathbf{k}}c_{\mathbf{k}\sigma}^\dagger c_{\mathbf{k}\sigma} + \sigma^x\sum_{\mathbf{k}\sigma}V_{\mathbf{k}}(c_{\mathbf{k}\sigma}^\dagger d_\sigma + \text{H.c.}) - \frac{U}{4}\sigma^z, \tag{34}$$

which describes a localized d level that hybridizes with a bath of conduction electrons. The sign of the hybridization depends on an Ising degree of freedom σ^x whose dynamics is controlled by a field $U/4$ in the z direction. Within DMFT, the bath parameters $\epsilon_{\mathbf{k}}$ and $V_{\mathbf{k}}$ are self-consistently determined [17]. Specifically, through the Hamiltonian, Eq. (34), we calculate the single-particle Green's function of the *physical* electron $\sigma^x d_\sigma$ in Matsubara frequencies:

$$G(i\omega_n) = -\int_0^\beta d\tau\, e^{i\omega_n\tau}\,\langle T_\tau[\sigma^x(\tau)\,d_\sigma(\tau)\sigma^x(0)\,d_\sigma^\dagger(0)]\rangle, \tag{35}$$

and we require that the self-consistency is reached when

$$\sum_{\mathbf{k}}\frac{V_{\mathbf{k}}^2}{i\omega_n - \epsilon_{\mathbf{k}}} = t^2 G(i\omega_n). \tag{36}$$

We emphasize that the self-consistency equation involves the physical electron $\sigma^x d_\sigma$, thus pseudofermions d_σ and Ising spins σ^x are both dynamical fields. These DMFT self-consistency equations are derived in the Appendix.

We shall focus hereafter on three dynamical quantities: the Green's function of the physical electron defined above, Eq. (35); the one of the auxiliary fermion d_σ,

$$G_d(i\omega_n) = -\int_0^\beta d\tau\, e^{i\omega_n\tau}\langle T_\tau[d_\sigma(\tau)d_\sigma^\dagger(0)]\rangle; \tag{37}$$

and finally the Ising spin Green's function

$$G_\sigma(i\Omega_\lambda) = -\int_0^\beta d\tau\, e^{i\Omega_\lambda\tau}\langle T_\tau[\sigma^x(\tau)\sigma^x(0)]\rangle, \tag{38}$$

where ω_n and Ω_λ are fermionic and bosonic Matsubara frequencies, respectively. The corresponding spectral functions are defined by the analytic continuation to the real axis, for

instance,

$$A(\omega) = -\frac{1}{\pi}\mathrm{Im}\, G(i\omega_n \to \omega + i0^+),$$

and similarly for $G_d(i\omega_n)$ and $G_\sigma(i\Omega_\lambda)$, to which we shall associate $A_d(\omega)$ and $A_\sigma(\omega)$, respectively.

The NRG calculations have been performed using discretization parameter $\Lambda = 2$, with twist averaging over $N_z = 8$ interleaved discretization grids. The calculations can be performed taking into account the spin $SU(2)$ symmetry and the axial charge (isospin) $SU(2)$ symmetry. The finite-temperature expectation values and dynamical quantities have been computed by the full-density-matrix algorithm [31,32] and the self-energy has been determined using the approach with an auxiliary Green's function defined for the physical electron operator [33]. Such calculations are highly reliable and can in principle be controllably improved by reducing the parameter Λ toward the continuum limit of $\Lambda = 1$, where they would become exact.

In order to reveal the spontaneous symmetry breaking, we shall add to the Hamiltonian, Eq. (34), a test field

$$\delta\mathcal{H} = -h_x\sigma^x, \tag{39}$$

and calculate the average of σ^x as $h_x \to 0$. Moreover, we shall separately discuss the solution at zero and at finite temperature.

A. $T = 0$ DMFT results

The impurity model, Eq. (34), without self-consistency and with a constant density of states of the bath was studied at zero temperature in Ref. [18]. It describes a dissipative two-level system [34], where the eigenstates of σ^x label the two levels and σ^z induces tunneling among them. The dissipative bath is actually sub-Ohmic so that the tunneling σ^z is irrelevant and the level localizes, i.e., $\langle\sigma^x\rangle \neq 0$ [18]. This case was argued to correspond to the metallic phase of the Hubbard model, Eq. (9). The issue is whether this is indeed true, namely, if the localization revealed by $\langle\sigma^x\rangle \neq 0$ survives the self-consistency condition, Eq. (36).

In Fig. 2 we show the spectral functions of the physical and auxiliary fermions, $A(\omega)$ and $A_d(\omega)$, black and red curves in the left panel, respectively, as well as of the Ising spin $A_\sigma(\omega)$, right panel, for different values of U. Several features are worth being highlighted. From the physical fermion spectral function $A(\omega)$ we can locate the Mott transition between $U/D = 2.8$ and 3, in full agreement with the direct studies of the Hubbard model [17]. The manifestations of such a transition in the behavior of the auxiliary fermion and the slave spin are quite interesting. The auxiliary fermion has a spectral function $A_d(\omega)$ resembling that of a resonant model that shrinks continuously approaching the Mott transition, above which its weight is concentrated in a δ peak that is not visible in the figure.

The Ising spin shows even more remarkable dynamical features. In the metallic phase the spectral function $A_\sigma(\omega)$ displays two peaks at the position of the Hubbard bands but also a linear component $A_\sigma(\omega) \sim \omega$ close to zero frequency. In other words, unlike in the mean-field solution, the Ising spectral function extends down to zero frequency. The linear low-frequency behavior occurs in an interval that shrinks as

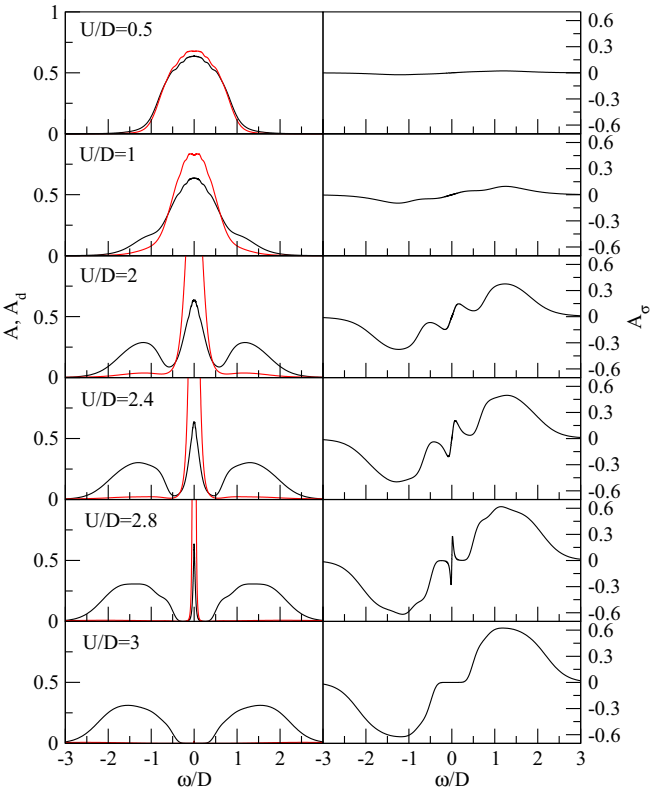

FIG. 2. (Color online) Left panels: Zero-temperature spectral functions of the physical and auxiliary fermions, $A(\omega)$ and $A_d(\omega)$, shown as black and red curves, respectively, for a range of U. Right panels: Corresponding Ising spin spectral functions $A_\sigma(\omega)$, which, being the imaginary part of a causal response function, is odd in frequency. For $U/D = 3$ the system is in the insulating phase.

the Mott transition is approached, and meanwhile the slope increases, just as we would expect to observe in the imaginary part of the physical-electron charge response function. Above the transition, this low-energy component disappears, and a gap opens in the spectrum. This is consistent with the picture of the Mott insulating state where the charge degrees of freedom freeze on a high-energy scale.

In Fig. 3(a) we plot the Ising magnetization $\langle\sigma^x\rangle$ as a function of an external test field h_x [see Eq. (39)] in the metallic phase at $U/D = 2.6$. We observe that $\langle\sigma^x\rangle$ approaches a finite value as $h_x \to 0$, thus revealing the spontaneous breaking of the Z_2 gauge symmetry. In the Mott insulating phase $\langle\sigma^x\rangle$ instead vanishes for $h_x \to 0$. It thus follows that $\langle\sigma^x\rangle$ is a legitimate order parameter of the zero-temperature Mott transition in the slave-spin language, finite in the metal and zero in the insulator, in qualitative agreement with the mean-field calculation.

In Fig. 3(b) we plot $\lim_{h_x\to 0}\langle\sigma_x\rangle$ as a function of U (black line). Its behavior is remarkably close to the $\sqrt{1 - U^2/U_c^2}$ dependence predicted by the static mean-field approximation (orange dashed line) [see Eq. (19)] provided that the actual numerically determined value $U_c = 2.97D$ is used rather than the static mean-field value of $U_c = 3.39D$. It is also instructive to compare the quasiparticle renormalization factor $Z = [1 - d\Re\Sigma(\omega)/d\omega]^{-1}$ (red line) with $\langle\sigma_x\rangle^2$ (blue dashed line) which is proportional to the pseudofermion bandwidth in the static

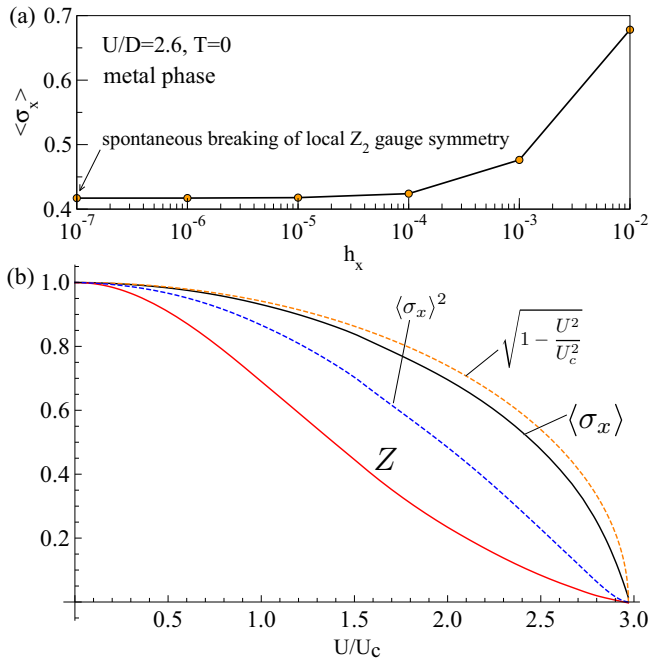

FIG. 3. (Color online) (a) Ising magnetization $\langle\sigma^x\rangle$ as a function of an external test field h_x in the metallic phase at $U/D = 2.6$ and at zero temperature. We note the finite value as $h_x \to 0$. (b) Zero-field Ising magnetization $\langle\sigma_x\rangle$ (full black line) and the quasiparticle renormalization factor (full red line) as a function of U. For comparison, we also plot $\langle\sigma_x\rangle^2$ (blue dashed line) and $\sqrt{1-U^2/U_c^2}$ (orange dashed line).

mean-field picture [see Eqs. (17)–(19)]. Although the slopes are different, both curves are linear close to the Mott transition point, i.e., $\langle\sigma_x\rangle^2 \propto Z$, confirming the intuitive picture that the Ising spin expectation value controls the bandwidth for the fermionic quasiparticles in the metal phase.

B. $T > 0$ DMFT results

The zero-temperature results demonstrate that the speculations based on the two-level system Hamiltonian, Eq. (34), are reliable. We observe that while at $T = 0$ a two-level system coupled to a sub-Ohmic bath localizes, at any $T \neq 0$ it does not, i.e., $\langle\sigma^x\rangle = 0$, $\forall T > 0$ [34]. The recovery of the gauge symmetry at finite temperature is evident in Fig. 4 where we show the slave-spin magnetization $\langle\sigma^x\rangle$ vs h_x in the metal (upper panel) for different temperatures. In the insulator (bottom panel), the magnetization for $h_x \to 0$ is practically zero at any temperature. In the metal, however, we observe the gradual onset of a finite order parameter as $T \to 0$ before $h_x \to 0$. This is further confirmed by the behavior of the zero-field slave-spin susceptibility, $\chi = d\langle\sigma_x\rangle/dh_x$. In the metal phase, for fixed and sufficiently small h_x the susceptibility is increasing as a power law T^{-1} in the range $T \gtrsim h_x$ before saturating for $T \ll h_x$. The saturated value of $\chi(T = 0)$ diverges as h_x^{-1}. In the insulator, the susceptibility at fixed h_x is weakly increasing with decreasing T and it saturates on the temperature scale of order bandwidth. The saturated value of $\chi(T = 0)$ does not depend on h_x in the insulator.

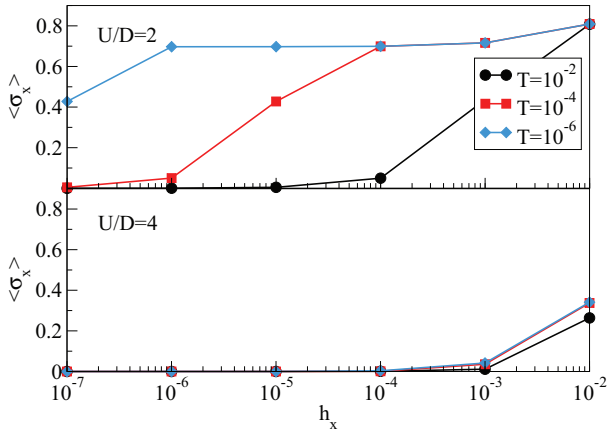

FIG. 4. (Color online) Ising magnetization $\langle\sigma^x\rangle$ as a function of an external test field h_x in the metallic phase at $U/D = 2$ (top panel) and the insulating one at $U/D = 4$ (bottom panel), for different temperatures.

The establishment of spontaneous symmetry breaking is also clear in Fig. 5, where we plot (at zero test field, $h_x = 0$) the correlation function of the Ising spin, i.e.,

$$C^{>}_{\rm spin}(\omega) = \frac{1}{Z}\sum_n e^{-\beta E_n}|\langle n|\sigma^x|m\rangle|^2\delta(\omega - E_m + E_n)$$
$$= \int_{-\infty}^{\infty} dt\, e^{i\omega t}\langle\,\sigma^x(t)\,\sigma^x(0)\,\rangle, \qquad (40)$$

which is better suited to capture the low-frequency singularity without the spectral weight cancellation due to broadening that affects more severely the (odd in frequency) Green's function $A_\sigma(\omega)$. We observe that $C^{>}_{\rm spin}(\omega)$ gradually develops a $\delta(\omega)$ peak as T decreases, which means that

$$\lim_{t\to\infty}\lim_{T\to 0}\langle\sigma^x(t)\sigma^x(0)\rangle \to \langle\sigma^x\rangle^2 > 0,$$

hence the spontaneous symmetry breaking [35].

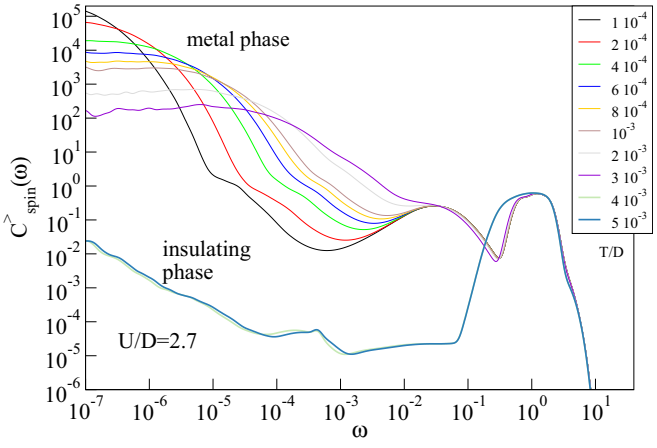

FIG. 5. (Color online) Correlation function $C^{>}_{\rm spin}(\omega)$ of the Ising operator σ^x at $U/D = 2.7$, i.e., in the metal phase not far from the transition, for different temperatures. We note the gradual emergence of a δ peak at $\omega = 0$ on decreasing the temperature toward $T = 0$.

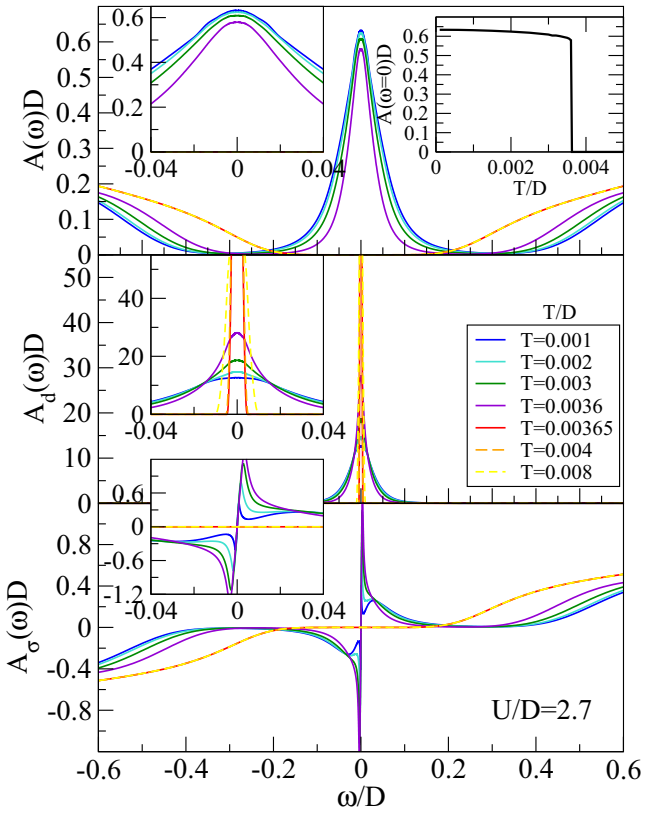

FIG. 6. (Color online) Spectral functions of the physical electron (top panel), of the auxiliary fermion (middle panel), and of the Ising spin (bottom panel) at $U = 2.7D$ upon increasing the temperature across the first-order metal-insulator transition. The insets show the close-ups to the low-frequency behavior. The right-hand inset in the top panel shows the density of states at the chemical potential of the physical electrons at $U = 2.7D$ upon increasing the temperature.

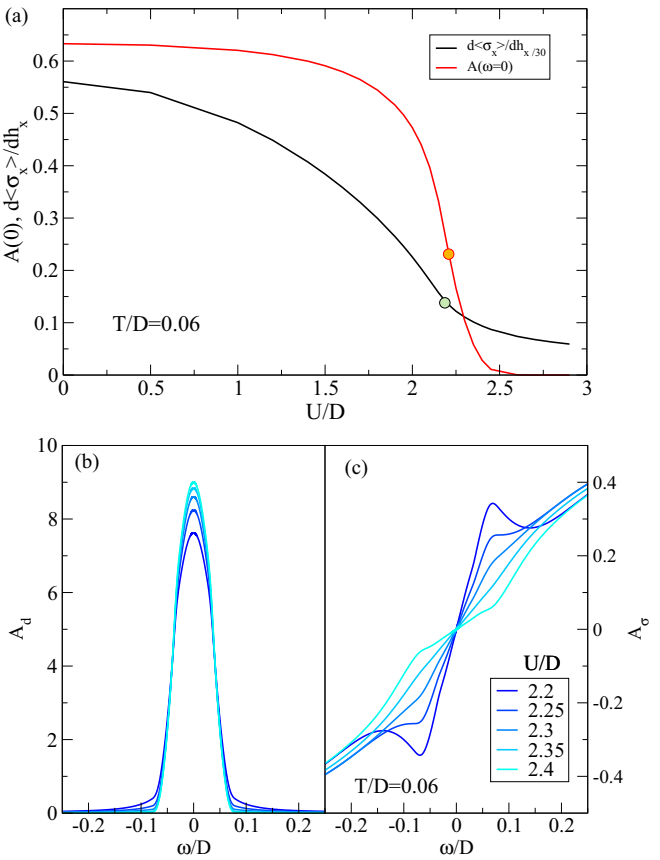

FIG. 7. (Color online) (a) Physical-electron spectral function intensity at $\omega = 0$ and the slave-spin susceptibility $d\langle\sigma_x\rangle/dh_x$ at constant temperature $T > T_c$ as functions of U. The circles indicate the inflection points on both curves that may serve as possible definitions of the crossover between the bad metal and the Mott insulator. (b) Auxiliary-fermion and (c) slave-spin spectral functions across the metal-insulator crossover.

In Fig. 6(a) we show the temperature evolution of the spectral functions $A(\omega)$, $A_d(\omega)$, and $A_\sigma(\omega)$ at $U = 2.7D$, when the system is in the metal phase at zero temperature and, upon heating, crosses the first-order transition and turns into a Mott insulator (see Fig. 1). The close-ups to the low-frequency behavior are shown as insets. We observe that, across the phase transition, the zero-frequency density of states of the physical electron jumps down from a finite to an extremely small value, as shown in detail in Fig. 6 (right inset to top panel), which is what one also obtains directly from the Hubbard model, Eq. (9).

The novelty here is represented by the behavior of the auxiliary fermion and slave-spin spectral functions. We observe that $A_d(\omega)$ does not change qualitatively across the transition; it always looks like the spectral function of a resonant level model, whose width and height simply jump at the transition.

More remarkable is the behavior of the slave-spin spectral function $A_\sigma(\omega)$. Until the system stays in the metal phase, $T \lesssim 0.0037D$, $A_\sigma(\omega) \sim \omega$ at small ω, with a slope that is practically temperature independent (see Fig. 6, bottom panel). Unlike at the zero-temperature Mott transition, the interval in which $A_\sigma(\omega) \sim \omega$ increases with temperature until, above the first-order transition, it suddenly disappears; all low-energy spectral weight is transferred at high energy (see Fig. 6), and a gap opens.

For $T > T_c \simeq 0.026D$, i.e., above the critical end point (see Fig. 1), there is no metal-insulator transition anymore upon increasing U; just a smooth crossover between a bad metal (large resistivity, increasing with T) and a Mott insulator (large but finite resistivity, decreasing with T). There is no unique definition of the crossover location, but it is empirically found that different choices, using either the spectral function, the resistivity, or the double occupancy, bring to almost coincident values (e.g., see Fig. 4 in Ref. [36]). We have found that in the slave-spin language the crossover also reveals itself by an inflection point in the slave-spin susceptibility $d\langle\sigma_x\rangle/dh_x$ [see Fig. 7(a)]. The evolution of spectral functions across the crossover is smooth, although we find a notable difference between auxiliary fermions and slave spins. The auxiliary-fermion spectrum changes only qualitatively: with increasing U the width of the peak narrows down and its height thus raises [see Fig. 7(b)]. Since the spin operators of auxiliary and physical fermions map onto each other, the above evolution simply represents the gradual formation of localized moments. On the contrary, the slave-spin spectrum, which describes charge degrees of freedom, shows a more

pronounced variation: the linear slope of the low-frequency component drops markedly [see Fig. 7(c)], signaling a rapid crossover from a gapless to a pseudogap regime.

C. Gauge-symmetry breaking's fate at $T > 0$

The previous results confirm the expectation that, as soon as $T > 0$, the Ising order parameter $\langle \sigma_i^x \rangle = 0$, in the sense that its expectation value in the presence of a test field h_x vanishes when $h_x \to 0$. To state this in a different manner, we have found that the 2^N degeneracy of each many-body excited eigenstate is not split linearly in the field strength h_x, unlike what happens for the ground state.

We observe that the model Hamiltonian, Eq. (11), which describes fermion and spin fields coupled in a gauge-invariant manner, lacks an explicit gauge field. The latter could be made explicit should we decouple the spin-fermion interaction through a Hubbard-Stratonovich transformation involving an auxiliary link variable that would just play the role of the gauge field. A question we may then ask ourselves is whether, even though the "matter" field, i.e., the Ising field σ_i^x, has vanishing expectation value, still the gauge field has a finite average value, as one would expect in a Z_2 gauge-Higgs theory [37–39]. In order to address this question we add to the Hamiltonian, Eq. (11), another source field

$$\delta\mathcal{H}_{\text{s-f}} = -\frac{h}{\sqrt{z}} \sum_{\langle i,j \rangle} \sum_{\sigma} (c_{i\sigma}^\dagger c_{j\sigma} + \text{H.c.}). \tag{41}$$

At finite h the gauge-variant operator $c_{i\sigma}^\dagger c_{j\sigma}$ acquires a finite expectation value, and accordingly, also $\langle \sigma_i^x \sigma_j^x \rangle$ becomes finite. Within the DMFT mapping onto an impurity model, the source term, Eq. (41), amounts to adding to Eq. (34) the additional term

$$\delta\mathcal{H}_{\text{imp}} = \sum_{\mathbf{k}\sigma} \epsilon_{f\mathbf{k}} f_{\mathbf{k}\sigma}^\dagger f_{\mathbf{k}\sigma} + \sum_{\mathbf{k}\sigma} V_{f\mathbf{k}} (f_{\mathbf{k}\sigma}^\dagger d_\sigma + \text{H.c.}), \tag{42}$$

which corresponds to hybridizing the impurity with another conduction channel f, and impose, besides Eq. (36), also

$$\sum_{\mathbf{k}} \frac{V_{f\mathbf{k}}^2}{i\omega_n - \epsilon_{f\mathbf{k}}} = h^2 G_d(i\omega_n). \tag{43}$$

The impurity model $\mathcal{H}_{\text{imp}} + \delta\mathcal{H}_{\text{imp}}$ supplemented by the self-consistency conditions, Eqs. (36) and (43), can still be solved by NRG, even though it now involves two channels of conduction electrons. The solution gives access to all local quantities of the original lattice Hamiltonian $\mathcal{H}_{\text{s-f}} + \delta\mathcal{H}_{\text{s-f}}$, both static and dynamic. However, in this more complicated situation we were not able to exploit the cavity method as in Ref. [17] and relate local quantities to nonlocal ones so to directly calculate $\langle c_{i\sigma}^\dagger c_{j\sigma} \rangle$. We thence opted for an indirect route and calculated the free energy of the impurity model $F_{\text{imp}}(h)$ as a function of the source field h, shown in Fig. 8 for different temperatures below (metal) and above (insulator) the Mott transition at $U = 2.7D$. However, even though the change that occurs at the finite temperature Mott transition is observable, the dependence on h is not regular enough to state unquestionably whether or not the impurity susceptibility diverges in the limit $h \to 0$. Therefore we cannot give any definite answer to the question about the finiteness of the gauge-field expectation value.

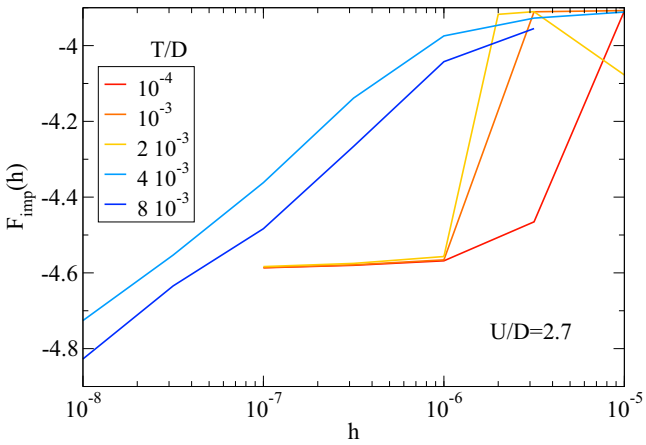

FIG. 8. (Color online) Impurity free energy for the model with the source term of Eq. (42). We plot the results vs h for a range of temperatures, both in the metallic and in the insulating phase.

IV. CONCLUSION

We have shown that the Mott metal-to-insulator transition in infinitely coordinated lattices can be faithfully reproduced by a model of fermions coupled in a Z_2 gauge-invariant manner to Ising spins in a transverse field. We very accurately solved such a model by dynamical mean-field theory using the numerical renormalization group as impurity solver, and found that gauge-symmetry breaking spontaneously occurs at zero temperature and corresponds to the metal phase in the original electronic model. The zero-temperature metal-to-insulator transition translates in this spin-fermion representation to the recovery of the Z_2 gauge symmetry, thus endowing the Mott transition of a genuine order parameter. Since we also found that gauge invariance is recovered at any, however small, finite temperature, we suspect that the Ising magnetization order parameter is closely related to the Fermi surface discontinuity in the quasiparticle distribution, which also disappears at any nonzero temperature. While the exact phase diagram agrees qualitatively well with that obtained by mean-field theory, the dynamical properties differ substantially. Indeed, contrary to mean field, we have found that the slave-spin spectral function is gapless everywhere in the metallic phase, where it shows a linear dependence at low frequency, and becomes gapped only in the Mott insulator. This is the case both at zero and at finite temperature, even though in the latter case the transition, for $T \lesssim T_c \simeq 0.026D$, or the crossover, above T_c, are not anymore related to the Ising spontaneous magnetization, which is zero for any $T \neq 0$. Our attempts to uncover the behavior of the gauge field, which is hidden in the theory, in order to better characterize the finite temperature phase transition/crossover were unfortunately not conclusive, even though the dynamical behavior of the auxiliary Ising fields notably changes across it.

ACKNOWLEDGMENTS

R.Ž. acknowledges the support of the Slovenian Research Agency (ARRS) under Program No. P1-0044. M.F. thanks G. Martinelli for useful discussions.

APPENDIX A: CAVITY CONSTRUCTION

In this Appendix we derive the DMFT equations for the spin-fermion model. We consider the Hamiltonian

$$\mathcal{H}_{\text{s-f}} = -\sum_{ij\sigma} t_{ij}\sigma_i^x\sigma_j^x c_{i\sigma}^\dagger c_{j\sigma} - \frac{U}{4}\sum_i \sigma_i^z. \tag{A1}$$

Here $t_{ij} = t/\sqrt{z}$ for nearest neighbors. We introduce the Grassman coherent states $c_i(\tau)$ for fermions and spin coherent states $\boldsymbol{\sigma}_i(\tau)$ for the Ising variables, where (suppressing the site index i for clarity)

$$\begin{aligned}
|\boldsymbol{\sigma}(\tau)\rangle &= \cos\frac{\theta(\tau)}{2}|\uparrow\rangle + e^{i\phi(\tau)}\sin\frac{\theta(\tau)}{2}|\downarrow\rangle,\\
\sigma^x(\tau) &= \langle\boldsymbol{\sigma}(\tau)|\sigma^x|\boldsymbol{\sigma}(\tau)\rangle = \sin\theta(\tau)\cos\phi(\tau),\\
\sigma^z(\tau) &= \langle\boldsymbol{\sigma}(\tau)|\sigma^z|\boldsymbol{\sigma}(\tau)\rangle = \cos\theta(\tau),
\end{aligned}$$

so that

$$\begin{aligned}
\langle\boldsymbol{\sigma}(\tau+d\tau)|\boldsymbol{\sigma}(\tau)\rangle &= \cos\frac{\theta(\tau+d\tau)}{2}\cos\frac{\theta(\tau)}{2} + e^{-i[\phi(\tau+d\tau)-\phi(\tau)]}\sin\frac{\theta(\tau+d\tau)}{2}\sin\frac{\theta(\tau)}{2}\\
&\simeq 1 - i\,\sin^2\frac{\theta(\tau)}{2}\frac{\partial\phi(\tau)}{\partial\tau} \simeq \exp\left[-i\,\sin^2\frac{\theta(\tau)}{2}\frac{\partial\phi(\tau)}{\partial\tau}\right].
\end{aligned}$$

The corresponding partition function is defined as

$$Z = \int\prod_{i\sigma}\mathcal{D}(\bar{c}_{i\sigma},c_{i\sigma})\prod_i\mathcal{D}(\theta_i,\phi_i)e^{-S}, \tag{A2}$$

with the action for Hamiltonian (A1) that reads

$$S = \int_0^\beta d\tau\left[\sum_{i\sigma}\bar{c}_{i\sigma}(\tau)\partial_\tau c_{i\sigma}(\tau) + \sum_i i\,\sin^2\frac{\theta_i(\tau)}{2}\partial_\tau\phi_i(\tau)\right] - \int_0^\beta d\tau\sum_{ij\sigma}t_{ij}\,\sigma_i^x(\tau)\sigma_j^x(\tau)\bar{c}_{i\sigma}(\tau)c_{j\sigma}(\tau) - \frac{U}{4}\int_0^\beta d\tau\sum_i\sigma_i^z(\tau). \tag{A3}$$

By tracing out all degrees of freedom except for site 0, we obtain the effective action as

$$\frac{1}{Z_{\text{eff}}}e^{-S_{\text{eff}}[\bar{c}_0,c_0,\theta_0,\phi_0]} \equiv \frac{1}{Z}\int\prod_{i\neq0,\sigma}\mathcal{D}(\bar{c}_{i\sigma},c_{i\sigma})\prod_{i\neq0}\mathcal{D}(\theta_i,\phi_i)e^{-S}. \tag{A4}$$

We split the action into three different parts, $S = S_0 + S_\Delta + S_{(0)}$. Here 0 indicates an arbitrary but fixed site of the lattice. S_0 is the local on-site part, $S_{(0)}$ is the lattice part with the site 0 removed, and S_Δ corresponds to the hopping part which connects S_0 and $S^{(0)}$:

$$S_0 = \int_0^\beta d\tau\left[\sum_\sigma\bar{c}_{0\sigma}(\tau)\partial_\tau c_{0\sigma}(\tau) + i\,\sin^2\frac{\theta_0(\tau)}{2}\partial_\tau\phi_0(\tau) - \frac{U}{4}\sigma_0^z(\tau)\right], \tag{A5}$$

$$S_\Delta = -\int_0^\beta d\tau\sum_{i\sigma}\sigma_0^x(\tau)\sigma_i^x(\tau)[t_{0i}\bar{c}_{0\sigma}(\tau)c_{i\sigma}(\tau) + t_{i0}\bar{c}_{i\sigma}(\tau)c_{0\sigma}(\tau)]. \tag{A6}$$

We define $\Delta_S(\tau)$ to be the integrand in the expression for S_Δ, i.e.,

$$\begin{aligned}
\Delta_S(\tau) &= -\frac{t}{\sqrt{z}}\sum_{\sigma,i\ \text{nn}\ 0}\sigma_0^x(\tau)\sigma_i^x(\tau)[\bar{c}_{0\sigma}(\tau)c_{i\sigma}(\tau) + \bar{c}_{i\sigma}(\tau)c_{0\sigma}(\tau)]\\
&= -\sum_{\sigma,i\ \text{nn}\ 0}\left[\frac{t}{\sqrt{z}}\sigma_0^x(\tau)\bar{c}_{0\sigma}(\tau)\right]\left[\sigma_i^x(\tau)c_{i\sigma}(\tau)\right] + \left[\sigma_i^x(\tau)\bar{c}_{i\sigma}(\tau)\right]\left[\frac{t}{\sqrt{z}}\sigma_0^x(\tau)c_{0\sigma}(\tau)\right].
\end{aligned} \tag{A7}$$

The form in the second line emphasizes that

$$\eta_i \equiv \frac{t}{\sqrt{z}}c_{0\sigma}\sigma_0^x \tag{A8}$$

will play the role of the source coupled to $\bar{c}_{i\sigma}\sigma_i^x$.

The partition function becomes

$$Z = \int \prod_{\sigma} \mathcal{D}(\bar{c}_{0\sigma}, c_{0\sigma}) \mathcal{D}(\theta_0, \phi_0) e^{-S_0} \int \prod_{\sigma, i\neq 0} \mathcal{D}(\bar{c}_{i\sigma}, c_{i\sigma}) \prod_{i\neq 0} \mathcal{D}(\theta_i, \phi_i) e^{-S_{(0)}} e^{-S_\Delta}$$
$$= Z^{(0)} \int \prod_{\sigma} \mathcal{D}(\bar{c}_{0\sigma}, c_{0\sigma}) \mathcal{D}(\theta_0, \phi_0) e^{-S_0} \langle e^{-S_\Delta} \rangle_{(0)}. \tag{A9}$$

Here $Z^{(0)}$ is the lattice partition function in the presence of the cavity,

$$Z^{(0)} = \int \prod_{i\neq 0, \sigma} \mathcal{D}(\bar{c}_{i\sigma}, c_{i\sigma}) \prod_{i\neq 0} \mathcal{D}(\theta_i, \phi_i) e^{-S_{(0)}} \tag{A10}$$

and the $\langle\,\rangle_{(0)}$ is an expectation value in the system with the site 0 removed. We expand

$$\langle e^{-S_\Delta} \rangle_{(0)} = 1 - \int_0^\beta d\tau \langle \Delta_S(\tau) \rangle_{(0)} + \frac{1}{2!} \int_0^\beta \int_0^\beta d\tau_1 \, d\tau_2 \langle T_\tau \Delta_S(\tau_1) \Delta_S(\tau_2) \rangle_{(0)} + \cdots . \tag{A11}$$

The integration over the degrees of freedom for $i \neq 0$ provides the generating functional of the connected Green's functions $G^{(0)}$:

$$S = S_0 + \sum_{n=1}^{\infty} \sum_{i_1, \ldots, i_n, j_1, \ldots, j_n} \int \eta^\dagger_{i_1}(\tau_{i_1}) \cdots \eta^\dagger_{i_n}(\tau_{i_n}) G^{(0)}_{i_1, \ldots, j_n}(\tau_{i_1}, \ldots, \tau_{i_n}, \tau_{j_1}, \ldots, \tau_{j_n}) \eta_{j_1}(\tau_{j_1}) \cdots \eta_{j_n}(\tau_{j_n}). \tag{A12}$$

In infinite dimensions ($z \to \infty$), only the second term remains, i.e., the nonzero contribution will come from the two-point Green's functions $\langle T_\tau \sigma^x_i(\tau_1) \sigma^x_j(\tau_2) c_{i\sigma}(\tau_1) \bar{c}_{j\sigma}(\tau_2) \rangle$.

The effective action thus becomes

$$S_{\text{eff}} = \int_0^\beta d\tau \left[\sum_\sigma \bar{c}_{0\sigma}(\tau) \partial_\tau c_{0\sigma}(\tau) + i \, \sin^2 \frac{\theta_0(\tau)}{2} \partial_\tau \phi_0(\tau) - \frac{U}{4} \sigma^z_0(\tau) \right] - \int_0^\beta d\tau \int_0^\beta d\tau' \sum_\sigma \bar{c}_{0\sigma}(\tau) \sigma^x_0(\tau) \Delta(\tau, \tau') \sigma^x_0(\tau') c_{0\sigma}(\tau'), \tag{A13}$$

with

$$\Delta(\tau, \tau') = \frac{t^2}{z} \sum_{i,j \text{ nn of } 0} G^{(0)}_{ij}(\tau, \tau'). \tag{A14}$$

Here $G^{(0)}$ is the Green's function for $\sigma^x_i c_{i\sigma}$ objects (these are, in fact, the *physical* electron operators) of the lattice with the site 0 removed. Specializing on the Bethe lattice where the neighbors of 0 are disconnected, only the $i = j$ terms remain and, furthermore, $G^{(0)}_{ii} = G_{ii}$. Finally, assuming a homogeneous solution, all neighbors i are equivalent and we finally obtain

$$\Delta(\tau, \tau') = t^2 G(\tau, \tau'). \tag{A15}$$

This fully defines the effective impurity model to be solved. We note again that it is the physical electron's Green's function G which enters the DMFT self-consistency loop, just like in the standard DMFT formulation.

[1] N. F. Mott, Proc. Phys. Soc. A **62**, 416 (1949).
[2] S. E. Barnes, J. Phys. F: Met. Phys. **6**, 1375 (1976).
[3] P. Coleman, Phys. Rev. B **29**, 3035 (1984).
[4] G. Kotliar and A. E. Ruckenstein, Phys. Rev. Lett. **57**, 1362 (1986).
[5] N. Read, J. Phys. C: Solid State Phys. **18**, 2651 (1985).
[6] N. E. Bickers, Rev. Mod. Phys. **59**, 845 (1987).
[7] E. Arrigoni, C. Castellani, R. Raimondi, and G. C. Strinati, Phys. Rev. B **50**, 2700 (1994).
[8] L. de'Medici, A. Georges, and S. Biermann, Phys. Rev. B **72**, 205124 (2005).
[9] S. D. Huber and A. Rüegg, Phys. Rev. Lett. **102**, 065301 (2009).
[10] A. Rüegg, S. D. Huber, and M. Sigrist, Phys. Rev. B **81**, 155118 (2010).
[11] M. Schiró and M. Fabrizio, Phys. Rev. B **83**, 165105 (2011).
[12] V. J. Emery, Phys. Rev. B **14**, 2989 (1976).
[13] E. H. Lieb, Phys. Rev. Lett. **62**, 1201 (1989).
[14] A. Taraphder and P. Coleman, Phys. Rev. Lett. **66**, 2814 (1991).
[15] R. Žitko and J. Bonča, Phys. Rev. B **74**, 224411 (2006).
[16] T. A. Costi and V. Zlatič, Phys. Rev. Lett. **108**, 036402 (2012).
[17] A. Georges, G. Kotliar, W. Krauth, and M. J. Rozenberg, Rev. Mod. Phys. **68**, 13 (1996).
[18] P. P. Baruselli and M. Fabrizio, Phys. Rev. B **85**, 073106 (2012).
[19] K. G. Wilson, Rev. Mod. Phys. **47**, 773 (1975).
[20] R. Bulla, T. A. Costi, and T. Pruschke, Rev. Mod. Phys. **80**, 395 (2008).
[21] S. Elitzur, Phys. Rev. D **12**, 3978 (1975).
[22] P. Maślanka, Acta Phys. Pol., B **19**, 269 (1988).

[23] H. Park, K. Haule, and G. Kotliar, Phys. Rev. Lett. **101**, 186403 (2008).
[24] M. J. Rozenberg, R. Chitra, and G. Kotliar, Phys. Rev. Lett. **83**, 3498 (1999).
[25] M. Fabrizio, in *New Materials for Thermoelectric Applications: Theory and Experiment*, edited by V. Zlatic and A. Hewson, NATO Science for Peace and Security Series B: Physics and Biophysics (Springer, Dordrecht, 2013), pp. 247–272.
[26] J. Bünemann, W. Weber, and F. Gebhard, Phys. Rev. B **57**, 6896 (1998).
[27] M. Fabrizio, Phys. Rev. B **76**, 165110 (2007).
[28] M. Schiró and M. Fabrizio, Phys. Rev. Lett. **105**, 076401 (2010).
[29] W.-S. Wang, X.-M. He, D. Wang, Q.-H. Wang, Z. D. Wang, and F. C. Zhang, Phys. Rev. B **82**, 125105 (2010).
[30] M. Sandri, M. Capone, and M. Fabrizio, Phys. Rev. B **87**, 205108 (2013).
[31] R. Peters, T. Pruschke, and F. B. Anders, Phys. Rev. B **74**, 245114 (2006).
[32] A. Weichselbaum and J. von Delft, Phys. Rev. Lett. **99**, 076402 (2007).
[33] R. Bulla, A. C. Hewson, and T. Pruschke, J. Phys.: Condens. Matter **10**, 8365 (1998).
[34] A. J. Leggett, S. Chakravarty, A. T. Dorsey, M. P. A. Fisher, A. Garg, and W. Zwerger, Rev. Mod. Phys. **59**, 1 (1987).
[35] In the NRG, it is difficult to reliably compute dynamical quantities in the frequency range $|\omega| \lesssim T$. In spite of this, the tendency towards the formation of a δ peak in the $T \to 0$ limit can be established.
[36] J. Vučičević, H. Terletska, D. Tanasković, and V. Dobrosavljević, Phys. Rev. B **88**, 075143 (2013).
[37] R. Balian, J. M. Drouffe, and C. Itzykson, Phys. Rev. D **10**, 3376 (1974).
[38] E. Brézin and J. M. Drouffe, Nucl. Phys. B **200**, 93 (1982).
[39] G. A. Jongeward, J. D. Stack, and C. Jayaprakash, Phys. Rev. D **21**, 3360 (1980).